

Joint Convexity of Error Probability in Blocklength and Transmit Power in the Finite Blocklength Regime

Yao Zhu, Yulin Hu*, Xiaopeng Yuan, M. Cenk Gursoy, H. Vincent Poor,
Anke Schmeink

Abstract

To support ultra-reliable and low-latency services for mission-critical applications, transmissions are usually carried via short blocklength codes, i.e., in the so-called finite blocklength (FBL) regime. Different from the infinite blocklength regime where transmissions are assumed to be arbitrarily reliable at the Shannon's capacity, the reliability and capacity performances of an FBL transmission are impacted by the coding blocklength. The relationship among reliability, coding rate, blocklength and channel quality has recently been characterized in the literature, considering the FBL performance model. In this paper, we follow this model, and prove the joint convexity of the FBL error probability with respect to blocklength and transmit power within a region of interest, as a key enabler for designing systems to achieve globally optimal performance levels. Moreover, we apply the joint convexity to general use cases and efficiently solve the joint optimization problem in the setting with multiple users. We also extend the applicability of the proposed approach by proving that the joint convexity still holds in fading channels, as well as in relaying networks. Via simulations, we validate our analytical results and demonstrate the advantage of leveraging the joint convexity compared to other commonly-applied approaches.

Index Terms

finite blocklength regime, error probability, resource allocation, joint design, convexity

This work was supported in part by the China National Key Research and Development Program under Grant 2021YFB2900301, in part by BMBF Germany in the program of "Souverän. Digital. Vernetzt." Joint Project 6G-RIC with project identification number 16KISK028, and in part by the U.S. National Science Foundation under Grant CNS-2128448.

Y. Zhu, Y. Hu, X. Yuan and A. Schmeink are with the Chair of Information Theory and Data Analytics, RWTH Aachen University, 52074 Aachen, Germany (e-mail: {zhu,hu,yuan,schmeink}@isek.rwth-aachen.de). M. C. Gursoy is with the Department of Electrical Engineering and Computer Science, Syracuse University, NY 13210, USA (e-mail: mcgursoy@syr.edu). H. V. Poor is with the Department of Electrical Engineering, Princeton University, Princeton, NJ 08544 USA (e-mail: poor@princeton.edu). *Y. Hu is the corresponding author.

I. INTRODUCTION

Supporting low-latency and ultra-reliability transmissions is crucial for wireless networks in order to enable novel mission-critical applications in real-time, such as vehicle-to-vehicle/infrastructure communications, augmented/virtual reality and factory automation [1], [2]. One of the key approaches to fulfill the stringent latency requirements of those applications is to employ short-packet communications carried out via finite blocklength (FBL) codes [3], [4]. In such FBL scenarios, the transmission error is no longer negligible, as a key departure from the so-called infinite blocklength (IBL) regime in which the transmissions are arbitrarily reliable at the rate of Shannon's capacity. In 2010, Polyanskiy *et al.*, in the landmark work [5], derived a closed-form expression of the decoding error probability in the FBL regime, when transmissions occur over a channel with additive white Gaussian noise (AWGN). It has been shown that the decoding error probability of FBL codes is positive even if the coding rate is less than the Shannon capacity, and this probability is higher when the blocklength gets shorter. Subsequently, the FBL performance characterization in [5] has been extended to Gilbert-Elliott channels [6], and quasi-static flat-fading channels [7], [8]. More recently, the FBL performance has been analytically investigated considering cooperative relay networks [9]–[12], non-orthogonal multiple access (NOMA) schemes [13]–[15], wireless power transfer [16], [17], system security [18] and green communications [19], [20].

Additionally, the design of future Internet-of-Things (IoT) networks calls for the support of massive access, also known as massive Machine Type Communications (mMTC), while guaranteeing the stringent latency and reliability requirements of each device [4]. Therefore, the short packet communications are likely to be carried out with FBL codes. Following the FBL model in [5] to characterize the accurate error probability performance, a set of optimal system designs has been provided for such low-latency multi-device networks via blocklength allocation [21], [22], power control [23]–[25] and transmission rate selection [26]. All the above designs address optimality with respect to a single factor/parameter, e.g., the blocklength, transmit power or the coding rate. However, it is practically more important to investigate multi-factor joint designs, in which, for instance, joint resource allocation with respect to both transmit power and blocklength is considered. A joint design via the optimization of multiple parameters leads to improved performance compared to single-factor design, and helps the network meet the critical requirements of different devices. Moreover, from a theoretical point of view, in comparison to a

single factor optimization, a joint design provides greater insights into the fundamental tradeoff among the considered factors and parameters especially in a multi-user scenario. Understanding such tradeoffs is particularly important in designing resource-limited networks (e.g., in terms of coding blocklength and transmit power) supporting multi-device low latency and ultra reliable transmissions.

A key challenge in obtaining the optimal solution of such a joint design is to characterize the principal properties (e.g., the joint convexity) of the design objective which involves complicated normal approximations [5]. In fact, the widely applied FBL performance metrics introduced in [5] have two characteristics that complicate the design and analysis. First, the expressions for the coding rate and error probability may not apply to extreme scenarios, e.g., with extremely low SNR or short blocklength. Secondly, the expressions for the FBL coding rate and error probability are significantly more complicated than the corresponding expression for the Shannon capacity, making model-based analytical derivations challenging. To address the first issue, existing studies usually assume that the values of the SNR and blocklength lie within certain regions of practical interest where the expressions of the performance metrics are applicable. To tackle the second difficulty, the original FBL model in [5] has been simplified in the following two ways: On the one hand, a linear approximation of the FBL error probability has been proposed to facilitate the analytical derivations [27], [28], especially when the system involves multiple fading channels [16], [17], [29] and random task arrivals [30]. On the other hand, instead of approximating the error expression, the channel dispersion can be simplified with a high SNR assumption [19], [31]–[33]. Recently, based on the above two approaches (by either assuming certain SNR and blocklength regions of practical interest or simplifying the FBL model), a set of designs is provided in [22], [34], [35], e.g., by optimizing with respect to multiple factors based on the concavity/convexity of the performance metric as a function of individual factors separately. R.2.7-6 In particular, based on the convexity of the performance metric as a function of each single parameter, multi-factor joint optimization problems have been addressed via an alternating search [22], [34], successive convex approximation [24] or integer convex optimization [18], [31], [35] (solving all single-parameter sub-problems with different feasible integer values of blocklength).

However, the aforementioned approaches face various challenges: the accuracy of a simplified FBL model [36] is often an issue, global optimum is difficult guarantee, and the computational complexity of solution search is usually high. Therefore, it is of interest to investigate the

joint convexity to characterize performance using the original FBL model with the normal approximation. In fact, although the joint convexity of the error probability approximation based on the original model can be observed (within certain regions of interest) in a set of existing works via numerical simulations [37]–[39], to the best of our knowledge, proving this joint convexity and determining such a region is still an open challenge.

In this paper, we study the joint convexity of error probability with respect to blocklength and transmit power based on the original FBL model in [5] and analyze its applicability in realistic multi-user scenarios. The main contributions of this paper can be summarized as follows:

- We first prove the joint convexity of the FBL error probability with respect to the transmit power and coding blocklength within a certain region of interest.
- We then study the general use case of joint convexity in a setting, in which we encounter a non-convex optimization problem due to a non-convex constraint, complicating the identification of efficient joint resource allocation strategies. By exploiting a novel variable substitution method, we reformulate the optimization problem, prove its convexity, and solve it optimally with low complexity compared to the commonly applied methods.
- To further extend the applicability of our results, we analyze two additional practical scenarios, one with a fading channel and the other involving a cooperative relaying system. We prove that the joint convexity still holds for both cases.
- Via simulations, we validate our analytical results and show the significant advantages of our proposed joint optimization approaches compared to benchmark schemes, emphasizing especially the scalability to networks with massively many devices.

The remainder of the paper is organized as follows. In Section II, we present the FBL model and introduce the preliminary concepts, formulations and approximations. The joint convexity is characterized in Section III. In Section IV, the use case of resource allocation is studied. The applicability of our results to other practical scenarios is investigated in Section V. Numerical results are presented in Section VI. Finally, we conclude the paper in Section VII. Several proofs are relegated to the Appendix.

II. FBL ERROR MODEL AND PRELIMINARY ANALYSIS

A. Error probability in the FBL regime

Consider a general wireless communication system with FBL codes, where the source transmits a data packet containing D bits using a codeword with blocklength m via a wireless link to a

receiver. Assume we have perfect channel state information and the channel gain z (including path-loss) is constant over the entire blocklength m . Then, the signal-to-noise ratio (SNR) of the received packet at the receiver is $\gamma = zp/\sigma^2$, where p is the transmit power and σ^2 represents the noise spectral density.

As the transmission is carried out in the FBL regime, i.e., the blocklength m is no longer sufficiently large to be considered infinite, the assumption of communicating arbitrarily reliably at the Shannon limit is no longer accurate. In other words, the transmission can be erroneous, even if the coding rate is less than the Shannon capacity. In particular, the maximal achievable transmission rate with target error probability ε_0 is given approximately by [5]

$$r^* \approx \mathcal{C}(\gamma) - \sqrt{\frac{V(\gamma)}{m}} Q^{-1}(\varepsilon_0), \quad (1)$$

where $\mathcal{C} = \log_2(1 + \gamma)$ is the Shannon capacity, and V is the channel dispersion [40]. In particular, we have $V = 1 - (1 + \gamma)^{-2}$ in a channel with fixed gain. Moreover, Q^{-1} is the inverse Q-function with $Q(x) = \int_x^\infty \frac{1}{\sqrt{2\pi}} e^{-\frac{t^2}{2}} dt$.

According to (1), we can also approximately characterize the (block) error probability with given transmission rate $r = \frac{D}{m}$ as follows:

$$\varepsilon = \mathcal{P}(\gamma, r, m) \approx Q\left(\sqrt{\frac{m}{V(\gamma)}}(\mathcal{C}(\gamma) - r)\log_e 2\right), \quad (2)$$

which provides a tight approximation on the error probability in the FBL regime, and has been widely applied [8]-[30]. In the remainder of the paper, we consider this expression as the FBL performance metric and characterize its convexity.

B. Preliminary Analysis via Additional Approximation Approaches

Although the Equation in (2) provides an accurate approximate formula for the error probability in the FBL regime, it is still analytically difficult to apply (2) in efficiently addressing the related optimization problems due to its non-convexity. In particular, ε is neither a convex nor a concave function with respect to either m or γ , since the Q-function itself initially behaves as a concave function for negative values of its argument and then becomes convex. To overcome this challenge, mainly two further approximation approaches have been applied in the literature:

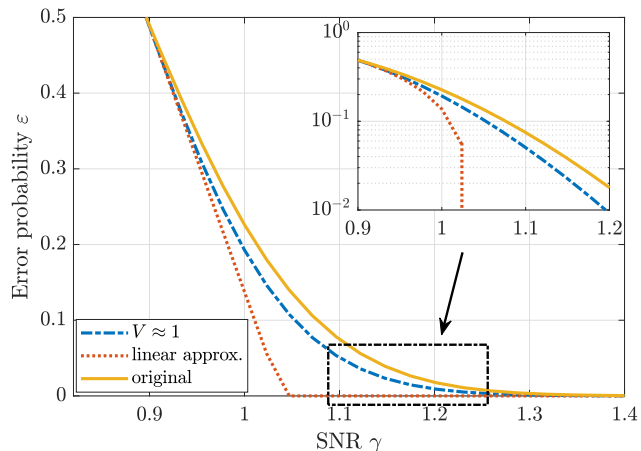


Fig. 1: Comparison of the error probability values computed by using the original expression in (2), linear approximation in (3), and the approximation obtained by letting $V \approx 1$. Note that the curves in the zoomed-in subfigure are convex in linear scale. The reason that they look non-convex is due to the fact that the subfigure is plotted in a logarithmic scale on the y-axis (in order to more clearly demonstrate the performance gap between the approximations and the original expression in a region with relatively low error probabilities).

1) *Linear approximation of ε* : By applying the linearization technique on the Q-function, the error probability in (2) can be approximated with three line segments [27], [28], i.e.,

$$\varepsilon \approx \begin{cases} 1, & \gamma < \alpha - \frac{1}{2\mu} \\ \frac{1}{2} - \mu(\gamma - \alpha), & \alpha - \frac{1}{2\mu} \leq \gamma \leq \alpha + \frac{1}{2\mu} \\ 0, & \gamma \geq \alpha + \frac{1}{2\mu}, \end{cases} \quad (3)$$

where $\alpha = e^r - 1$ and $\mu = -\sqrt{\frac{m}{2\pi(e^{2r}-1)}}$. Due to the simplicity of the expression, it has been widely applied in the literature, especially when dealing with fading channels [16], [17], [30].

However, the major drawback of such an approximation lies in the performance difference compared with (2). In particular, the approximation is tight when the error probability is relatively high, whereas the gap becomes significant when one enters the regime of reliable transmission with low error probabilities as shown in Fig. 1. In other words, the more reliable the transmission is, the less accurate the approximation becomes, which is counter to the purpose of studying the FBL model. For instance, enabling ultra-reliable low-latency communication (URLLC) services demands an error probability as low as 10^{-5} , for which the linear approximation is unable to accurately represent the actual error probability, as indicated in Fig. 1. Therefore, the applicability of such an approximation is weakened when we aim at investigating the reliability performance.

2) *Constant approximation of V* : Focusing on relatively reliable transmissions only, we can narrow the region of coding rates by assuming that $r \leq \mathcal{C}$. In particular, note that the sign of the

argument of the Q-function $Q(x)$ is determined by the sign of $\sqrt{\frac{m}{V}}(\mathcal{C} - r)$. Therefore, if $r \leq \mathcal{C}$ does not hold, we have $x < 0$, resulting in $\varepsilon = Q(x) > 0.5$, which is too high to be of interest in practical applications requiring high reliability. In the regime with $r \leq \mathcal{C}$, the Q-function $Q(x)$ is convex with respect to x . However, similar convex properties of ε with respect to other variables, e.g., m or γ , are still obscure due to the complicated dependencies within (2). To simplify the expression, the channel dispersion V in the AWGN channel can be approximated as a constant instead of being expressed as a function of SNR [31]–[33], i.e., $V \approx 1$.

However, it should be pointed out that the approximation is only accurate when the SNR is high and becomes loose in the medium range of SNR as shown in Fig. 1, which is still within the region of interest. Especially when we are dealing with the error probability instead of the maximal achievable coding rate, the performance gap is non-negligible. In fact, $V \approx 1$ implies that the SNR $\gamma \gg 1$, which could be a strong assumption that oversimplifies the influence of γ [6]. Therefore, it is worthwhile to utilize (2) directly without further approximations. Moreover, to enable the joint resource allocation approach with respect to both blocklength and power, the characterization can be more impactful if we are able to establish the joint convexity. In view of this, we analyze the convexity of ε in detail in the following section.

III. CHARACTERIZATION OF THE CONVEXITY OF ERROR PROBABILITY

Recall that we are interested in the tail behavior of the system [1], i.e., the transmissions are reliable with error probability $\varepsilon \leq \varepsilon_{\max} \ll 1$. In this regime, the performance cannot be guaranteed if the SNR is extremely low and/or the transmission rate is higher than the Shannon capacity. Therefore, in the considered work, we assume that $\varepsilon \leq \varepsilon_{\max} = 0.1$, $\gamma \geq \gamma_{\text{th}} = 0$ dB and $\mathcal{C}(\gamma) \geq r$ always hold to facilitate the derivations. Furthermore, we assume that the integer constraint on the blocklength can be relaxed*, i.e., from $m \in \mathbb{Z}_+$ to $m \in \mathbb{R}_+$. Then, we can establish the following lemma to characterize the convexity of ε in the regime of interest:

Lemma 1. *Consider an FBL transmission with conditions $\varepsilon \leq \varepsilon_{\max}$, $\gamma \geq 1$ and $\mathcal{C}(\gamma) \geq r$. The error probability is jointly convex in blocklength and transmit power, i.e., ε is convex in (m, p) ,*

We can obtain the integer solution of m by comparing the possible integer neighborhood of the non-integer solution, i.e., $m_{\text{int}} = \arg \min_{m \in \{\lfloor m^ \rfloor, \lceil m^* \rceil\}} f(m)$, where m^* is the non-integer optimal solution and f is the objective function.

if

$$r > \frac{2}{\ln 2(9(\gamma+1)^2-1)} \left(-2\gamma^2 - 4\gamma + \sqrt{4(\gamma^2+2\gamma)^2 + \frac{2}{5}(9(\gamma+1)^2-1)\ln^2(\gamma+1)} \right) \quad (4)$$

or more strictly

$$\gamma \geq \max \left\{ \frac{1}{5r \ln 2}, \frac{8}{45r^2 \ln^2 2} \right\}. \quad (5)$$

A sketch of the proof is as follows (a detailed proof is provided in Appendix A):

- 1) We first prove the convexity and monotonically decreasing property of error probability ε with respect to $w = \sqrt{\frac{m}{V(\gamma)}}(\mathcal{C}(\gamma) - \frac{D}{m}) \ln 2$.
- 2) Then we prove that the upper-left element in the Hessian matrix \mathbf{H} of w over m and γ is non-negative.
- 3) The determinant of the Hessian matrix is expressed in terms of a set of auxiliary functions, where the sign of each of them is proven to be non-negative under the condition in (4).
- 4) The condition in (5) is also shown to provide an intuitive physical meaning.

Remark: Numerically, the condition (4) is fulfilled if $r = \frac{D}{m} \geq 0.0448$ [bits/blocklength], which is true for most practical FBL applications in the region of interest. For the extreme case, a more intuitive condition (5) can be applied to provide the condition between SNR γ , namely Shannon capacity $\mathcal{C}(\gamma)$, and coding rate r to guarantee the convexity[†]. In other words, it indicates a maximal blocklength constraint with given information bits. It is worth mentioning that Lemma 1 is also valid for the cases with the linear approximation of ε and constant approximation of V , for which we can relax the constraint (4) and $\gamma > 1$.

By applying this characterization of convexity, we can now efficiently solve various joint optimization problems involving the error probability. To illustrate this, let a K -th order polynomial with non-negative coefficients to be the general error probability penalty/cost function $f(\mathbf{m}, \mathbf{p})$ in terms of blocklength $\mathbf{m} = \{m_1, \dots, m_N\}$ and normalized transmit power $\mathbf{p} = \{p_1, \dots, p_N\} = \{\gamma_1, \dots, \gamma_N\}$, each with N variables. We further denote by $\varepsilon_i(m_i, p_i)$ the FBL error probability with respect to m_i and p_i . Given these, we can express the penalty function $f(\mathbf{m}, \mathbf{p})$ as

$$f(\mathbf{m}, \mathbf{p}) = \sum_{k=1}^K \sum_{i=1}^N a_{i,k} \varepsilon_i^k(m_i, p_i), \quad (6)$$

[†]In fact, (2) is only accurate if the SNR is greater than 1 and coding rate is sufficiently high [36]. In the remainder of the paper, we assume that condition (4) is implicitly fulfilled.

with $a_{i,k} \geq 0$ denoting the non-negative coefficients. Then, we have the following corollary to characterize the expression.

Corollary 1. *The penalty function $f(\mathbf{m}, \mathbf{p})$ is also jointly convex in (\mathbf{m}, \mathbf{p}) under the conditions $\varepsilon_i \leq \varepsilon_{\max}$, $\gamma_i \geq 1$ and $\mathcal{C}(\gamma_i) \geq r_i$.*

Proof. For the k -th term $a_k \varepsilon_i^k$ of the polynomial, we have

$$\frac{\partial^2(a_k \varepsilon_i^k)}{\partial \mathbf{m}^2} = \frac{\partial^2(a_k \varepsilon_i^k)}{\partial m_i^2} = \begin{cases} a_k k(k-1) \varepsilon_i^{k-2} \left(\frac{\partial \varepsilon_i}{\partial m_i}\right)^2 + a_k k \varepsilon_i^{k-1} \frac{\partial^2 \varepsilon_i}{\partial m_i^2}, & \text{if } k \geq 2 \\ a_k \frac{\partial^2 \varepsilon_i}{\partial m_i^2}, & \text{if } k = 1 \\ 0, & \text{if } k = 0 \end{cases} \geq 0. \quad (7)$$

Similarly, we can show that

$$\frac{\partial^2(a_k \varepsilon_i^k)}{\partial \mathbf{m}^2} \frac{\partial^2(a_k \varepsilon_i^k)}{\partial \mathbf{p}^2} - \left(\frac{\partial^2(a_k \varepsilon_i^k)}{\partial \mathbf{m} \partial \mathbf{p}}\right)^2 \geq 0, \quad (8)$$

regardless of the value of k . Therefore, $a_k \varepsilon_i^k$ is jointly convex in \mathbf{m} and \mathbf{p} . As a sum of convex functions, $f(\mathbf{m}, \mathbf{p})$ is also jointly convex in \mathbf{m} and \mathbf{p} . ■

Based on Corollary 1, any problem that has the following form within a convex feasible regime is convex:

$$\underset{\mathbf{m}, \mathbf{p}}{\text{minimize}} \quad f(\mathbf{m}, \mathbf{p}) \quad (9a)$$

$$\text{subject to} \quad \varepsilon_i \leq \varepsilon_{\max}, \forall i = 1, \dots, N, \quad (9b)$$

$$p_{\min} \leq p_i \leq p_{\max}, \forall i = 1, \dots, N, \quad (9c)$$

$$0 \leq m_i \leq m_{\max}, \forall i = 1, \dots, N. \quad (9d)$$

Clearly, as a convex problem, Problem (9) can be efficiently solved. On the other hand, it should be pointed out that the constraints of Problem (9) are general and can be loose, while many practical scenarios have more specific and strict constraints which are possibly non-convex. For example, constraints that include coupled variables, such as total energy consumption restrictions, are non-convex. To demonstrate how our analytical results in Lemma 1 and Corollary 1 facilitate the joint optimal design with practical and non-convex constraints, in the next section we analyze a general use case that is encountered frequently when dealing with multi-factor resource allocation with FBL codes.

IV. USE CASE: JOINT RESOURCE ALLOCATION

Consider a general multi-user scenario [22], [31], where a set of low-latency and reliable transmissions of N user equipments (UEs) are carried out via orthogonal multiple access, e.g., time-division multiple access (TDMA) or orthogonal frequency-division multiple access (OFDMA)[‡]. In particular, the transmission consists of N slots with blocklength $\mathbf{m} = \{m_1, \dots, m_N\}$, in which the server transmits packets with sizes of $\mathbf{D} = \{D_1, \dots, D_N\}$ information bits using normalized transmit power $\mathbf{p} = \{p_1, \dots, p_N\} = \{\gamma_1, \dots, \gamma_N\}$ to N UEs, respectively. We define $i \in \mathcal{N}$ as the index of a user and \mathcal{N} is the index set. Furthermore, the total available energy consumption is constrained by E and total available blocklength by M . We aim at minimizing the maximal error probability among those UEs by jointly optimizing blocklength and transmit power for each UE. To ensure the quality of transmission, the error probability of each transmission is below a threshold ε_{\max} while the SNR for each user is greater than a threshold $\gamma_{\text{th}} \geq 1$. Then, the problem can be formulated as follows

$$\underset{\mathbf{m}, \mathbf{p}}{\text{minimize}} \quad \max\{\varepsilon_i\} \quad (10a)$$

$$\text{subject to} \quad \sum_{i=1}^N m_i \leq M, \quad (10b)$$

$$\sum_{i=1}^N m_i p_i \leq E, \quad (10c)$$

$$\varepsilon_i \leq \varepsilon_{\max}, \forall i \in \mathcal{N}, \quad (10d)$$

$$\gamma_i \geq \gamma_{\text{th}}, \forall i \in \mathcal{N}. \quad (10e)$$

The objective function is jointly convex in \mathbf{m} and \mathbf{p} according to Lemma 1, while the constraint (10c) is non-convex. Hence, problem (10) is non-convex in its current form. In the following, we address this non-convex problem via different strategies. In particular, we first provide an optimal solution via a variable substitution method. Meanwhile, an alternating search and an integer search (both of which are based on the convex features of a single variable) are presented as benchmarks. It should be pointed out that these benchmarks are also the state-of-the-art approaches to provide multi-factor designs we discussed in Section I. At the end of the section, a comparison among all three approaches is provided to show the performance

[‡]We assume that the channels are frequency-flat [31], [41].

advantages of applying the characterized joint convexity in terms of optimality, complexity and scalability.

A. Solution Based on Joint Convexity

In particular, $\sum_{i=1}^N m_i p_i \leq E$ is a non-convex constraint, since both m_i and p_i are optimization variables, i.e., we jointly optimize the blocklength and transmit power. To address this issue without compromising the constraint (e.g., by fixing one of the variables or decomposing the constraint as $m_i p_i \leq E_{\max,i}, \forall i \in \mathcal{N}$), we exploit the following variable substitution method: Let $m_i = \frac{1}{a_i}$ and $p_i = b_i^2$, for $i \in \mathcal{N}$. Therefore, we can reformulate problem (10) with new variables \mathbf{a} and \mathbf{b} as follows

$$\begin{aligned} & \underset{\mathbf{a}, \mathbf{b}}{\text{minimize}} && \max_{i \in \mathcal{N}} \{\varepsilon_i\} \end{aligned} \tag{11a}$$

$$\text{subject to} \quad \sum_{i=1}^N \frac{1}{a_i} \leq M, \tag{11b}$$

$$\sum_{i=1}^N \frac{b_i^2}{a_i} \leq E, \tag{11c}$$

$$\varepsilon_i \leq \varepsilon_{\max}, \quad \forall i \in \mathcal{N}, \tag{11d}$$

$$\gamma_i \geq \gamma_{\text{th}}, \quad \forall i \in \mathcal{N}. \tag{11e}$$

It is trivial to prove the convexity of the reformulated constraint (11c), since it is the sum of N convex functions. Therefore, we focus on the convexity of ε_i . Due to the substitution of variables, Lemma 1 should be revised, since it is no longer sufficient in proving the joint convexity. To this end, we exploit the following lemma to characterize the objective function:

Lemma 2. *The objective function of problem (11) is jointly convex in \mathbf{a} and \mathbf{b} within the feasible set defined as $\varepsilon_i \leq \varepsilon_{\max}$ and $\gamma_i \geq \gamma_{\text{th}}, \forall i \in \mathcal{N}$.*

Proof. See Appendix B. ■

According to Lemma 2, problem (11) is a convex problem and can be solved efficiently by standard convex programming methods.

Although we consider the maximal error probability as our objective function, it should be pointed out that Lemma 2 can also be applied with other objectives. For instance, we can take total energy consumption, i.e., $\sum_{i=1}^N m_i p_i$, or effective throughput, i.e., $\sum_{i=1}^N D_i(1 - \varepsilon_i)$, as the

objective function. However, the exact design of the metric for the resource allocation problem is out of the main scope of this paper.

As a comparison, we also provide two other potential approaches that only leverage the individual convexity with respect to a single variable to solve the problem. Then, we discuss the advantage of the solutions based on joint convexity with respect to optimality, complexity and scalability.

B. Approaches Based on Individual Convexity

1) *Integer convex optimization*: Recall that the blocklength m_i is an integer variable and total available blocklength in the practical system is always limited. Therefore, the original problem (10) can be decomposed into $\frac{(M-1)!}{(M-N)!}$ sub-problems with fixed $\mathbf{m} = \mathbf{m}^o$ where \mathbf{m}^o is an element in the set of possible blocklength allocation combinations \mathcal{M} , i.e.,

$$\underset{\mathbf{p}}{\text{minimize}} \quad \max_i \{\varepsilon_i\} \quad (12a)$$

$$\text{subject to} \quad \mathbf{m} = \mathbf{m}^o, \quad (12b)$$

$$\sum_i^N m_i p_i \leq E, \quad (12c)$$

$$\varepsilon_i \leq \varepsilon_{\max}, \gamma_i \geq \gamma_{\text{th}}, \forall i \in \mathcal{N}. \quad (12d)$$

As proven in Lemma 1, ε_i is convex in \mathbf{p} and the rest of the constraints are either affine or convex. Therefore, the original problem becomes essentially an integer convex optimization problem.

2) *Iterative search*: Similar to fixing \mathbf{m} , we can also decompose the original problem by fixing $\mathbf{p} = \mathbf{p}^o$, i.e.,

$$\underset{\mathbf{m}}{\text{minimize}} \quad \max_i \{\varepsilon_i\} \quad (13a)$$

$$\text{subject to} \quad \mathbf{p} = \mathbf{p}^o, \quad (13b)$$

$$\sum_{i=1}^N m_i \leq M, \quad (13c)$$

$$\sum_i^N m_i p_i \leq E, \quad (13d)$$

$$\varepsilon_i \leq \varepsilon_{\max}, \gamma_i \geq \gamma_{\text{th}}, \forall i \in \mathcal{N}. \quad (13e)$$

Since both sub-problems (12) and (13) are convex, we can also solve the resource allocation problem in an alternating fashion. In particular, for each iteration k , we fix $\mathbf{p} = \mathbf{p}^{(k-1)}$ and

obtain $\mathbf{m}^{(k)}$ by solving Problem 13 optimally. Then, we fix $\mathbf{m} = \mathbf{m}^{(k)}$ and obtain $\mathbf{p}^{(k)}$ by solving Problem 12 optimally. We set $\mathbf{p}^{(0)}$ as the initial value for the first iteration. We repeat the above iterative procedure until convergence, and the convergence rate is linear with computational complexity $\mathcal{O}(2N^2)$ [42].

C. Comparison

Although all three aforementioned approaches are able to provide (sub-)optimal solutions for the considered joint resource allocation problem, they are quite different regarding their optimality, computational complexity and scalability:

- **Joint convex optimization:** One of the major advantages of this algorithm is its ability to provide an optimal solution with the low computational complexity of $\mathcal{O}(4N^2)$ while guaranteeing global optimality. Moreover, this approach is also scalable to support massive device access in low-latency IoT networks, since the complexity only has a second-order polynomial growth rate in N .
- **Integer convex optimization:** The globally optimal solution can be found by comparing the solutions of each decomposed sub-problem with all possible \mathbf{m}^o in \mathcal{M} , resulting in a computational complexity of $\mathcal{O}\left(\frac{(M-1)!}{(M-N)!}N^2\right)$, which is the major drawback of this approach. Specifically, the complexity increases exponentially with the available blocklength and number of UEs. This is especially prohibitive when the number of connected UEs is high.
- **Iterative search:** Recall that the complexity of iterative search is $\mathcal{O}(2N^2)$. Therefore, the advantage of iterative search is the low complexity compared to the integer convex programming. However, the solution obtained with this method is only sub-optimal and highly depends on the initialization. To improve the performance, one can run the algorithm multiple times with randomly chosen initial values. However, this increases the overall complexity and still cannot guarantee global optimality. Furthermore, the cost also grows further when the number of users, N , increases due to the larger space from which the initial value needs to be selected.

To elucidate the comparison, we list the properties of all three methods in terms of optimality, complexity and scalability in Table I.

	Convexity	Optimality	Complexity	Scalability
Joint convex optimization	joint	globally optimal	low	yes
Integer convex optimization	partial	globally optimal	high	no
Iterative search	partial	sub-optimal	low	conditional

TABLE I: Properties of three optimization approaches. Green highlighting indicates the best performance among the three candidates. The joint convex optimization shows significant advantages compared with other two common approaches in both theoretical perspectives, i.e., convexity and optimality, as well as practical perspectives, i.e., complexity and scalability. In particular, the joint convex optimization approach can optimally solve Problem (10) due to the joint convexity proven by Lemma 1 and 2. Therefore, the complexity is as low as $\mathcal{O}(4N^2)$. It implies that the joint convex optimization is scalable, which is critical to support massive connectivity.

V. EXTENSIONS TO FADING CHANNELS AND RELAY NETWORKS

In this section, we further extend and apply our analytical results to more specific scenarios in which the formulated problems are more complicated and precluding the direct use of our analytical findings in previous sections. In particular, we first investigate the joint convexity in a fading channel instead of the static channel. In this case, the error probability expression involves the fading distribution, and differs from the normal approximation in (2). Next, we consider a two-hop relaying system, where the overall error is influenced by the error of two links. Therefore, the overall error probability consists of the product of two dependent error probabilities, which increases the difficulty in establishing the convexity of the error probability. We demonstrate that our analytical results can also facilitate the analysis of joint convexity for both extensions.

A. Fading Channel

In the previous section, joint convexity is proven under the assumption of a static channel with perfect CSI knowledge. Now, let us consider a general quasi-static fading channel, the distribution of which follows central limit theorem, e.g., Rayleigh fading or Nakagami fading. In particular, the channel gain z (including the path-loss) is constant during each transmission with coding blocklength m but varies from one transmission to the next. Then, the expression of error probability in (2) is reformulated as

$$\mathbb{E}_z[\varepsilon] = \int_0^\infty \varepsilon f_Z(z) dz \quad (14)$$

where $f_Z(\cdot)$ denotes the probability density function (PDF) of the fading.

First, we still assume that perfect CSI is available before the considered transmission frame. Therefore, we are able to adjust the blocklength and power in each transmission. Then, the error probability for any single transmission with known z can still be evaluated by (2), unless

the channel gain is lower than the threshold z_{th} such that Shannon capacity is lower than the transmission rate even with maximal available blocklength M_{max} and maximal transmit power P_{max} , i.e., $\mathcal{C}(P_{\text{max}} | z \leq z_{\text{th}}) < \frac{D}{M_{\text{max}}}$. We further assume that the packets are dropped in transmissions with those parameters [32], i.e., $\varepsilon(m, p | z < z_{\text{th}}) = 1$. Then, the (expected) error probability over the fading channel is given by

$$\mathbb{E}_z[\varepsilon] = \int_0^{z_{\text{th}}} \varepsilon(m, p|z) f_Z(z) dz + \int_{z_{\text{th}}}^{\infty} \varepsilon(m, p|z) f_Z(z) dz. \quad (15)$$

Note that the fading is quasi-static. Then, let $z(\phi)$ denote an arbitrary channel state, where $\phi = \{1, \dots, \Phi\}$. Now, (15) can be further approximated as

$$\mathbb{E}_z[\varepsilon] \approx \sum_{\phi=1}^{\Phi} \varepsilon(m(\phi), p(\phi) | z = z(\phi)) f_Z(z(\phi)) \Delta\phi, \quad (16)$$

where $\Delta\phi = 1/\Phi$ is the channel quantization level. As $\Phi \rightarrow \infty$, i.e., $\Delta\phi \rightarrow 0$, the approximation becomes accurate. Then, we have following corollary to characterize the joint convexity:

Corollary 2. *The error probability over a quasi-static fading channel as given by $\mathbb{E}_z[\varepsilon]$ in (16) is also jointly convex in the blocklength and transmit power in each slot, i.e., as a function of $\mathbf{m} = \{m(1), \dots, m(\Phi)\}$ and $\mathbf{p} = \{p(1), \dots, p(\Phi)\}$.*

Proof. Note that $\mathbb{E}_z[\varepsilon]$ is a weighted sum of the error probabilities under each state $z(\phi)$. In the case of $z(\phi) \leq z_{\text{th}}$, we have

$$\frac{\partial^2 \varepsilon(m(\phi), p(\phi) | z = z(\phi)) f_Z(z(\phi))}{\partial(\mathbf{m}, \mathbf{p})^2} = 0. \quad (17)$$

Moreover, in the case of $z(\phi) > z_{\text{th}}$, according to Lemma 1, we have

$$\frac{\partial^2 \varepsilon(m(\phi), p(\phi) | z = z(\phi)) f_Z(z(\phi))}{\partial(\mathbf{m}, \mathbf{p})^2} = f_Z(z(\phi)) \frac{\partial^2 \varepsilon(m(\phi), p(\phi) | z = z(\phi))}{\partial(m(\phi), p(\phi))^2} \geq 0. \quad (18)$$

Hence, as a sum of convex functions, $\mathbb{E}_z[\varepsilon]$ is also convex. ■

However, CSI may not always available or the cost of gaining perfect CSI may be too high. In view of this, we consider a fading scenario where we only have the average CSI. Therefore, we are unable to adjust blocklength and transmit power in each transmission. In such scenarios, the instantaneous error probability may higher than 0.5 if the channel is sufficiently weak, i.e., coding rate is greater than Shannon capacity. To address this issue, following our previous work [43], we denote \bar{z} the medium of channel gain and \bar{z}_{th} the threshold so that the coding rate is just

lower than the instantaneous Shannon capacity. For any reliable transmission with $\varepsilon \leq \varepsilon_{\max}$, i.e., $0 \leq \bar{z}_{\text{th}} \leq \bar{z}$, we have following corollary to characterize the convexity:

Corollary 3. *In a reliable transmission, the convexity of $\mathbb{E}[\varepsilon]$ with respect to blocklength m or transmit power p is still valid.*

Proof. Let x presents blocklength m or transmit power p . For the second derivative of (14), we have

$$\frac{\partial^2 \mathbb{E}[\varepsilon]}{\partial x^2} = \int_0^{\bar{z}_{\text{th}}} \frac{\partial^2 \varepsilon}{\partial x^2} f_Z(z) dz + \underbrace{\int_{\bar{z}_{\text{th}}}^{\bar{z}} \frac{\partial^2 \varepsilon}{\partial x^2} f_Z(z) dz}_{\geq 0} + \underbrace{\int_{\bar{z}}^{\infty} \frac{\partial^2 \varepsilon}{\partial x^2} f_Z(z) dz}_{\geq 0}. \quad (19)$$

The last two terms are non-negative since the integral is the sum of the second derivative of error probability over $f_Z(z)$, which has been proven as convex in Lemma 1. However, the sign of the first term is still nondeterministic.

Note that \bar{z} is the median of the channel gain. The cumulative distribution function (CDF) follows

$$\int_{\bar{z}_{\text{th}}}^{\infty} f_Z(z) dz \geq \int_{\bar{z}}^{\infty} f_Z(z) dz = \int_0^{\bar{z}} f_Z(z) dz = \frac{1}{2} \geq \int_0^{\bar{z}_{\text{th}}} f_Z(z) dz. \quad (20)$$

It also holds that $\bar{z}_{\text{th}} \leq \bar{z}$. Hence, we have the following inequality:

$$\int_{\bar{z}_{\text{th}}}^{\infty} \frac{\partial^2 \varepsilon}{\partial x^2} dz \geq \left| \int_0^{\bar{z}_{\text{th}}} \frac{\partial^2 \varepsilon}{\partial x^2} dz \right|. \quad (21)$$

with multiplication of both sides in (20) and (21), the following inequality holds:

$$\int_{\bar{z}}^{\infty} \det \mathbf{H}(\varepsilon) f_Z(z) dz \geq \left| \int_0^{\bar{z}_{\text{th}}} \det \mathbf{H}(\varepsilon) f_Z(z) dz \right|. \quad (22)$$

It implies that (19) is non-negative. as a result, the convexity of $\mathbb{E}[\varepsilon]$ with respect to m or p holds. ■

Based on above discussion, we can conclude that the convexity still holds for both cases with fading channel. However, they are handled differently in the optimization according to the scenarios. On one hand, if we have perfect CSI, we should optimize the blocklength and transmit power in each slot (or each N slots, if we have N users). On the other hand, if we only have average CSI, the best we can do is to target at the long-term error probability and optimize the blocklength and transmit power with iterative search. However, it only has to be done once

for every slot. Nevertheless, all analytical results in previous sections are also applicable for quasi-static fading channel.

B. Cooperative Relaying

Cooperative relaying is one of the most efficient methods to mitigate fading by exploiting the spatial diversity and providing better channel quality. Thus, it is of interest to extend our results also to the typical two-hop relaying system. In particular, consider a relaying system, where the source (considered as node 1) transmits a data packet of D bits through a relay node (considered as node 2) to the destination. Assuming that the relay employs the decode-and-forward protocol, the channel in each hop experiences block fading, and perfect CSI is available, the error probability in each hop is given by

$$\varepsilon_i = \mathcal{P}(p_i, \frac{D}{m_i}, m_i), \quad (23)$$

where p_i is the normalized transmit power of hop i and m_i is the blocklength. Since the packet is transmitted forward through all nodes, an error occurs if the transmission in any hop fails, i.e., the (approximated) overall error probability can be written as

$$\varepsilon_O = \varepsilon_1 + (1 - \varepsilon_1)\varepsilon_2 = \varepsilon_1 + \varepsilon_2 - \varepsilon_1\varepsilon_2. \quad (24)$$

We aim at minimizing the overall error probability by jointly optimizing the blocklength and the transmit power for each hop while ensuring that the error probability of each hop is below the threshold ε_{\max} . Then, the optimization problem is given by

$$\begin{aligned} & \underset{\mathbf{m}, \mathbf{p}}{\text{minimize}} && \varepsilon_O && (25a) \\ & \text{subject to} && (10b) - (10e) \end{aligned}$$

Hence, the above optimization problem has essentially the same form of Problem (10) with the different objective function ε_O . However, Lemma 1 cannot be directly applied due to the second order term $\varepsilon_1\varepsilon_2$ in the objective function. In fact, in most existing works that study relay system with FBL codes [37], [44], [45], the term $\varepsilon_1\varepsilon_2$ is ignored. This may be inaccurate for the practical system, e.g., one of the hop has weak channel gain in a fading channel scenario. Therefore, we provide the following lemma to characterize the joint convexity of the overall error probability without ignoring $\varepsilon_1\varepsilon_2$.

Lemma 3. *The overall error probability ε_O is jointly convex in \mathbf{m} and \mathbf{p} within the feasible set defined as $\varepsilon_i \leq \varepsilon_{\max}$ and $\gamma_i \geq \gamma_{\text{th}}$, $\forall i \in \mathcal{N}$.*

Proof. We first define $w_i = \sqrt{\frac{m}{V(\gamma_i)}}(\mathcal{C}(\gamma_i) - \frac{D}{m}) \ln 2$, with which the overall error probability can be expressed as $\varepsilon_O = Q(w_1) + Q(w_2) - Q(w_1)Q(w_2)$. Note that $\varepsilon_1 = Q(w_1)$ and $\varepsilon_2 = Q(w_2)$. Then, we first show that the overall error probability ε_O is jointly convex in w_1 and w_2 . The Hessian matrix of ε_O with respect to w_1 and w_2 is given by

$$\hat{\mathbf{H}} = \begin{pmatrix} \frac{\partial^2 \varepsilon_O}{\partial w_1^2} & \frac{\partial^2 \varepsilon_O}{\partial w_1 \partial w_2} \\ \frac{\partial^2 \varepsilon_O}{\partial w_2 \partial w_1} & \frac{\partial^2 \varepsilon_O}{\partial w_2^2} \end{pmatrix}. \quad (26)$$

Clearly, the upper-left element in matrix $\hat{\mathbf{H}}$ can be expressed as

$$\frac{\partial^2 \varepsilon_O}{\partial w_1^2} = (1 - Q(w_2)) \frac{w_1}{\sqrt{2\pi}} e^{-\frac{w_1^2}{2}} \geq 0. \quad (27)$$

The above inequality holds due to the fact that $\varepsilon_2 = Q(w_2) \ll 1$ and $w_1 \geq 0$, which follows from $\varepsilon_1 = Q(w_1) \ll 1$. Similarly, we have for the lower-right element in $\hat{\mathbf{H}}$,

$$\frac{\partial^2 \varepsilon_O}{\partial w_2^2} = (1 - Q(w_1)) \frac{w_2}{\sqrt{2\pi}} e^{-\frac{w_2^2}{2}} \geq 0. \quad (28)$$

With the remaining elements formulated as

$$\frac{\partial^2 \varepsilon_O}{\partial w_1 \partial w_2} = \frac{\partial^2 \varepsilon_O}{\partial w_2 \partial w_1} = -\frac{1}{2\pi} e^{-\frac{w_1^2}{2} - \frac{w_2^2}{2}}, \quad (29)$$

we can obtain the determinant of matrix $\hat{\mathbf{H}}$ as

$$\begin{aligned} \det(\hat{\mathbf{H}}) &= (1 - Q(w_1))(1 - Q(w_2)) \frac{w_1 w_2}{2\pi} e^{-\frac{w_1^2}{2} - \frac{w_2^2}{2}} - \frac{1}{4\pi^2} e^{-w_1^2 - w_2^2} \\ &= \frac{1}{2\pi} e^{-\frac{w_1^2}{2} - \frac{w_2^2}{2}} \left(w_1 w_2 (1 - \varepsilon_O) - \frac{1}{2\pi} e^{-\frac{w_1^2}{2} - \frac{w_2^2}{2}} \right) \\ &\geq \frac{1}{2\pi} e^{-\frac{w_1^2}{2} - \frac{w_2^2}{2}} \left(1.2^2 (1 - \varepsilon_O) - \frac{1}{2\pi} e^{-1.2^2} \right) \geq 0, \end{aligned} \quad (30)$$

where the inequality holds due to the fact that $\varepsilon_i \leq \varepsilon_{\max} \ll 1$ and $w_1, w_2 \geq 1.2$. Moreover, e^{-x^2} is a monotonically decreasing function with respect to x . Therefore, we have proven that the overall error probability ε_O is jointly convex in w_1 and w_2 .

Note that when w_1 (or w_2) becomes larger, we will obtain a lower error probability ε_1 (or ε_2), and the overall error probability ε_O will also be lower. In other words, the overall error probability ε_O is a decreasing function of both w_1 and w_2 . On the other hand, according to Lemma 1, it has been proven that w_i is jointly concave in blocklength m_i and SNR γ_i , i.e., jointly concave in m_i and p_i . Therefore, we can conclude that the overall error probability is jointly convex in blocklength m_i and power p_i , i.e., jointly convex in \mathbf{m} and \mathbf{p} . \blacksquare

With Lemma 3, Problem (25) can also be reformulated by replacing $m_i = \frac{1}{b_i}$ and $p_i = a_i^2$ in a similar way as in Problem (11) in Section IV. Then, it can be easily solved as a convex problem. It is worth to mention that the joint convexity we characterized in Lemma 3 can also be applied to other scenarios, where the multiplication of error probabilities involved, such as the error probability in NOMA schemes and retransmission schemes.

VI. NUMERICAL RESULTS

In this section, we further validate our analytical characterizations via numerical results. We also show the advantage of leveraging the joint convexity compared to traditional approaches in the existing works presented as benchmarks. Unless specifically mentioned otherwise, the setup of the simulations is as follows: We set the total available blocklength as $M = 800$ [chn.use]. The normalized total energy budget as $E = 2400$ [W·chn.use]. The packet size is set as $D_i = 480$ [bits]. In such case, the bandwidth and transmission time interval is normalized to the unit value. Moreover, The path-loss is normalized to 1 and the channels are set to experience block-fading and i.i.d. with $h_n \sim \mathcal{N}(0, 1)$ while the noise spectral density $\sigma^2 = 0.01$. The error probability threshold is set as $\varepsilon_{\max} = 0.1$.

Parameter	Notation	Value
Total available blocklength	M	800 [chn.use]
(Normalized) total energy budget	E	2400 [W·chn.use]
Channel of user i	h_i	$\sim \mathcal{N}(0, 1)$
Noise spectral density	σ^2	0.01
Error probability threshold	ε_{\max}	0.1
SNR threshold	γ_{th}	1

TABLE II: parameter setups in the numerical simulations

We first illustrate the feasible set according to Lemma 1 in Fig. 2. We plot the heat map with respect to transmission rate r and SNR γ . The color indicates the value of the decoding error probability at that point, while the regimes without color or with transparent color are infeasible. We also plot the zoomed-in view of the boundary of condition (4). As discussed in previous sections, the area outside of the boundary is tiny and is not of interest considering the practical scenarios due to the extremely low transmission rates $r < 0.04$. On the other hand, the upper white area is the regime where $\mathcal{C} \leq r$, which also belongs to the non-convex set as we discussed in Section II, where the Q-function is always greater 0.5, i.e., $Q(x) \geq 0.5, \forall x \leq 0$.

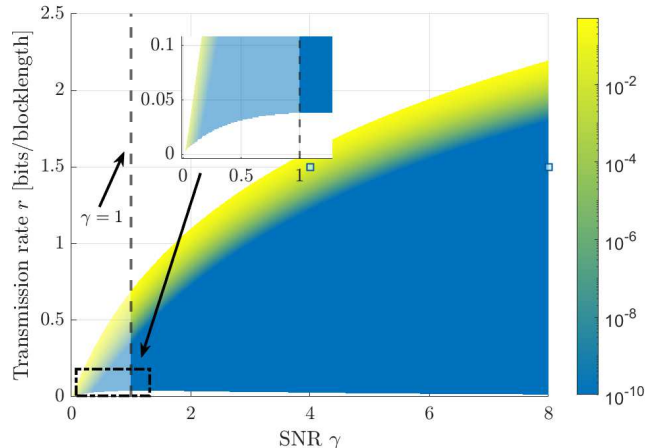


Fig. 2: Feasible set of the joint convexity for error probability in FBL regime. The color represents the value of $\varepsilon(\gamma, D, m)$. The zoom-in figure shows the boundary of condition (4).

Furthermore, recall that we consider the reliable transmission with a reasonable SNR threshold $\gamma \geq 1$. Therefore, the feasible regime is suitable for most practical application scenarios.

Next, we investigate the impact of transmit power p and blocklength m by showing the error probability against one of the variables while varying another, respectively. To present the influence of the channel model, we also plot ε for both static channel and (slow) fading channel in Fig. 3. Specifically, we analyze the error probability in (2) in terms of instantaneous SNR in the static channels and error probability in (14) in terms of average SNR in fading channels. Overall, we can observe that the curves are initially concave then convex in both p and m , taking the same shape as the Q-function regardless of whether static or fading channels are considered. This observation confirms our analytical results in Corollary 2.

However, above figures only investigate the convexity of the error probability with a single user. To further provide insight on the joint convexity in practical scenarios with two users, we plot in Fig. 4 the maximal error probability $\max_i \varepsilon_i$ against blocklength m_1 and transmit power p_1 of user 1, as well as the new set of variables a_1 and b_1 . As a comparison, both the 3D plot of $\max_i \varepsilon_i$ and the corresponding heat map are provided. It should be pointed out that the visible area of the figure represents the feasible set of Problem (10). As discussed in Section IV, ε_i is jointly convex in p_i and m_i , which is confirmed by the 3D plot in Fig. 4b. Therefore, the constraint $\varepsilon_i \leq \varepsilon_{\max}$ is also convex, with which the feasible set is bounded by the bottom line in Fig. 4a. However, the energy constraint $m_1 p_1 + m_2 p_2 \leq E$ is non-convex due to the multiplication of two variables, which results in a non-convex boundary depicted by the upper

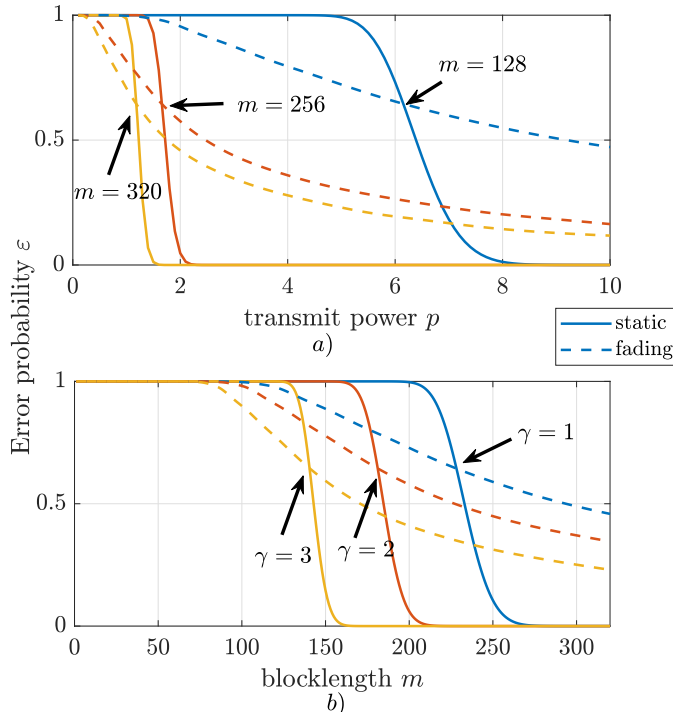


Fig. 3: Decoding error probability ε against a) transmit power p ; b) blocklength m in various setups. Both static channel with instantaneous SNR (solid lines) and fading channel with average SNR (dash lines) are plotted.

line in Fig. 4a. To tackle this issue, we let $a_i = \frac{1}{m_i}$ and $b_i = \sqrt{p_i}$. Then, the energy constraint becomes convex, while the convexity of ε_i is maintained. As a result, we have a jointly convex objective function (plotted in Fig. 4d) with a convex feasible set (shown as the intersection of two boundaries in Fig. 4c). These phenomena confirm our analytical results in Lemma 2.

Furthermore, we show the advantage of our proposed joint optimization solution by comparing the results with integer search and alternating search. In particular, we plot the total error probability against total available blocklength M with various total energy constraints in Fig. 5. Overall, the error probability decreases exponentially when we increase the total available blocklength M for all curves. However, we can observe significant performance gap between different approaches. On one hand, the proposed joint optimization design outperforms the alternating search method. It reveals the major disadvantage of alternating search. Specifically, the alternating search only offers sub-optimal solutions while our design is able to guarantee the global optimum. Moreover, longer total available blocklength M or smaller energy budget, i.e., lower power per blocklength, also enlarges the difference. This implies that alternating search may provide an acceptable solution if the interplay of those two variables has only a weak

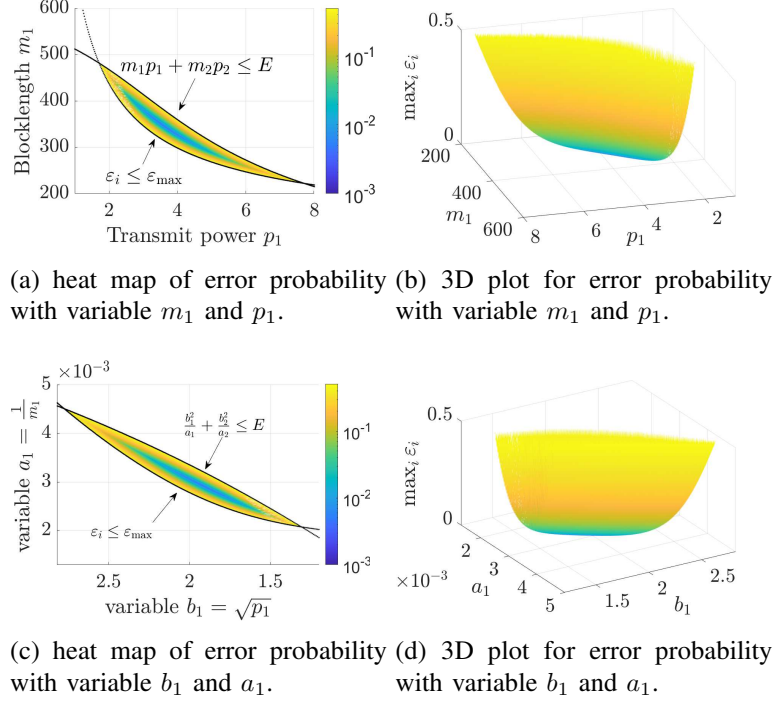


Fig. 4: maximal error probability $\max_i \varepsilon_i$ with constraint (10e) and (11c) against corresponding m_1 and p_1 , as well as $b_1 = \frac{1}{p_1}$ and $a_1 = \sqrt{m_1}$.

influence on the system and can be approximately decoupled, e.g., the channels of UEs are homogeneous. On the other hand, we observe that the performance of integer search (almost) matches the performance of joint optimization. In fact, both approaches can achieve the globally optimal solution. However, it should be emphasized that, although the integer search can provide globally optimal solution theoretically, it becomes computationally infeasible in practice for large IoT network scenarios, where massive number of sensor devices is involved due to the low computational efficiency.

Another important parameter influencing the system performance is the transmitted data size \mathbf{D} , which is investigated in Fig. 6. In particular, we plot the maximum error probability against average data size \bar{D} with 5 users. The data size is heterogeneous and follows a fixed ratio, i.e., $\mathbf{D} = \{0.8\bar{D}, 0.9\bar{D}, \bar{D}, 1.1\bar{D}, 1.2\bar{D}\}$ and $\sum_{i=1}^5 D_i = 5\bar{D}$. We also illustrate the performance difference between all three approaches in setups with varying total available blocklength $M = \{1000, 1250, 1500\}$. Clearly, increasing the average data size \bar{D} significantly increases the error probability. Moreover, we can also observe that there exists clearly a trade-off between the data size limitation that the system is able to support and the total available resources (available

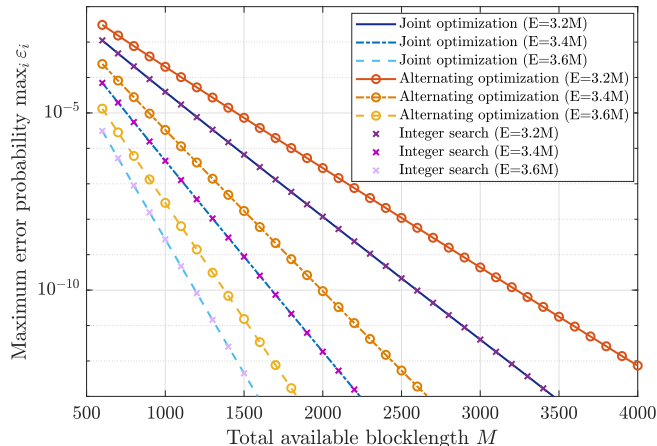


Fig. 5: Total error probability versus total available blocklength M . Performance comparison between our solution obtained with joint convexity feature, integer search and alternating search in various setups.

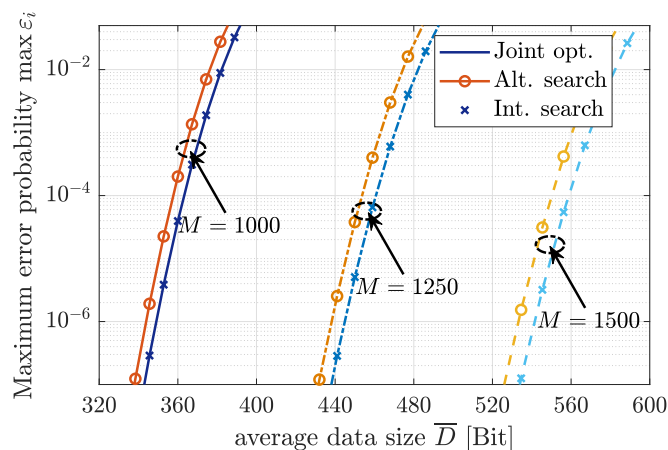


Fig. 6: Maximum error probability versus average data size \bar{D} with various total available blocklength M . Data size for each user is set as $\mathbf{D} = \{0.8\bar{D}, 0.9\bar{D}, \bar{D}, 1.1\bar{D}, 1.2\bar{D}\}$.

blocklength in this case). For example, for a target error probability of 10^{-4} , only $\bar{D} = 355$ bits can be transmitted with $M = 1000$. Meanwhile, we can transmit up to $\bar{D} = 540$ bits with $M = 1500$ at the same error level. From Fig 6, we also obtain similar observations as in Fig 5, i.e., joint optimization and integer search are able to provide better results than alternating search. Interestingly, the influence of \bar{D} on the performance gain between the global optimum (obtained via joint optimization and integer search) and the local optimum (obtained via alternating search) is insignificant. Therefore, the applicability of those approaches remains the same regardless of \bar{D} .

Finally, we evaluate the impact of the channel gain on the performance. Specifically, simula-

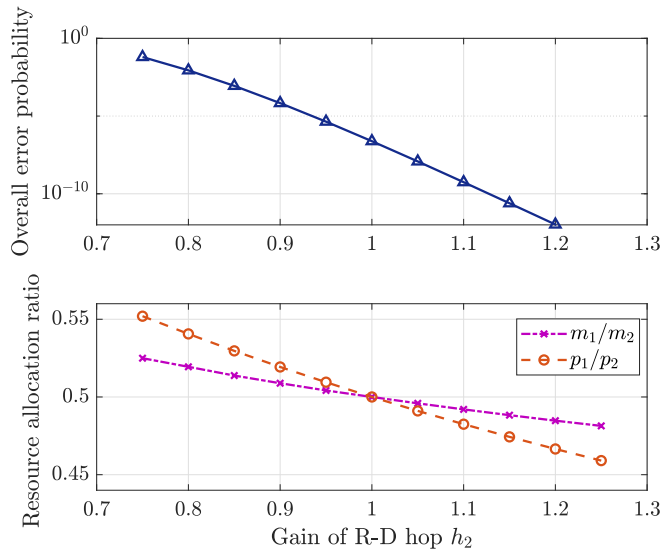


Fig. 7: Optimal overall error probability ε_O^* and optimal resource allocation ratio $\{\frac{m_1}{m_2}, \frac{p_1}{p_2}\}$ against channel gain of the second hop h_2 under the two hop relaying system.

tions are carried out considering a two-hop relaying system, where the overall error probability ε_O is determined by the combination of error probability in each hop $\varepsilon_1(m_1, p_1)$ and $\varepsilon_2(m_2, p_2)$. Fig 7 illustrates the optimal overall error probability ε_O^* and optimal resource allocation ratio $\{\frac{m_1}{m_2}, \frac{p_1}{p_2}\}$ versus the channel gain of the second hop h_2 , i.e., the gain between the relay and destination. Meanwhile, we set the channel gain between the source and relay as constant, i.e., $h_1 = 1$. The optimal solutions are obtained via our proposed joint optimization approach, i.e., the solutions are globally optimal. As expected, increasing the channel gain results in the decrease of ε_O^* . Since ε_O is a combination of ε_1 and ε_2 , the optimal resource allocation scheme is to distribute the blocklength and transmit power so that the performance is balanced in both hops. For instance, when $h_1 = h_2 = 1$, we have $m_1 = m_2$ and $p_1 = p_2$. This provides us insight on resource allocation in a homogeneous system. Specifically, when the users are considered as homogeneous (or if no information is available), an effective approach is to uniformly allocate the radio resources to each user.

VII. CONCLUSION

In this work, we have investigated the fundamental characteristics of the FBL error probability to enable joint optimization designs for reliable transmissions. We have proved the joint convexity of the error probability with respect to transmit power and blocklength within a certain region of practical interest. We have also studied a general use case with a non-convex joint optimization

problem in a multi-user scenario. By exploiting the variable substitution method, we have reformulated the problem as a convex problem and discussed the advantages of such an approach compared to other commonly applied methods. To further extend the applicability of this work, we have considered the joint convexity in two more practical scenarios, i.e., in fading channels and in cooperative relaying. In particular, we proved that the joint convexity still holds for these two scenarios. Via simulations, we have validated our analytical results and demonstrated the performance gain of our proposed approaches compared to benchmarks.

APPENDIX A

PROOF OF LEMMA 1

To facilitate the analysis, we first let $w = \sqrt{\frac{m}{V(\gamma)}}(\mathcal{C}(\gamma) - \frac{D}{m}) \ln 2$. As a result, the error probability can be rewritten as a composite function $\varepsilon = \varepsilon(w(\gamma, m))$. By taking the first and second derivatives of the error probability ε with respect to w , we have

$$\frac{\partial \varepsilon}{\partial w} = \frac{\partial \left(\int_w^\infty \frac{1}{\sqrt{2\pi}} e^{-\frac{t^2}{2}} dt \right)}{\partial w} = -\frac{1}{\sqrt{2\pi}} e^{-\frac{w^2}{2}} < 0, \quad (31)$$

$$\frac{\partial^2 \varepsilon}{\partial w^2} = \frac{w}{\sqrt{2\pi}} e^{-\frac{w^2}{2}} \geq 0. \quad (32)$$

The above inequalities hold due to the fact that w is always non-negative in the considered high-reliability scenario where $\mathcal{C}(\gamma) \geq r$. Clearly, the error probability ε is convex and monotonically decreasing in w within the considered regime, i.e., $w \geq 0$ ($\mathcal{C}(\gamma) \geq r$). Therefore, the joint convexity of ε in γ and m can be proved if we can prove that the auxiliary variable w is jointly concave with respect to γ and m .

Next, to prove the joint concavity of w in m and γ , we show that the Hessian matrix \mathbf{H} of auxiliary variable w is negative semi-definite, where the Hessian matrix \mathbf{H} can be expressed as

$$\mathbf{H} = \begin{pmatrix} \frac{\partial^2 w}{\partial m^2} & \frac{\partial^2 w}{\partial m \partial \gamma} \\ \frac{\partial^2 w}{\partial \gamma \partial m} & \frac{\partial^2 w}{\partial \gamma^2} \end{pmatrix}. \quad (33)$$

Subsequently, we investigate each component in matrix \mathbf{H} . On the one hand, for the partial derivatives of w with respect to m , we have

$$\frac{\partial w}{\partial m} = \frac{1}{2} m^{-\frac{1}{2}} V^{-\frac{1}{2}} \mathcal{C} \ln 2 + \frac{1}{2} m^{-\frac{3}{2}} V^{-\frac{1}{2}} D \ln 2 \geq 0, \quad (34)$$

$$\frac{\partial^2 w}{\partial m^2} = -\frac{1}{4} m^{-\frac{3}{2}} V^{-\frac{1}{2}} \mathcal{C} \ln 2 - \frac{3}{4} m^{-\frac{5}{2}} V^{-\frac{1}{2}} D \ln 2 \leq 0, \quad (35)$$

and therefore the term w is concave in blocklength m .

On the other hand, the partial derivative of w with respect to SNR γ is given by

$$\frac{\partial w}{\partial \gamma} = \frac{m^{\frac{1}{2}} V^{-\frac{1}{2}}}{(\gamma^2 + 2\gamma)(\gamma + 1)} \underbrace{(\gamma^2 + 2\gamma - \ln(\gamma + 1))}_{\Delta_1} + \frac{1}{2} m^{-\frac{1}{2}} V^{-\frac{3}{2}} D \ln 2 \frac{2}{(1 + \gamma)^3}, \quad (36)$$

where Δ_1 is a function of SNR γ . In addition, the derivative of Δ_1 with respect to γ is given by $\frac{\partial \Delta_1}{\partial \gamma} = 2\gamma + 2 - \frac{1}{\gamma + 1}$, which is monotonically increasing in $\gamma \geq 1$, so that we have $\frac{\partial \Delta_1}{\partial \gamma} \geq 3.5 > 0$ when $\gamma \geq 1$. Hence, we can also obtain that $\Delta_1 \geq \Delta_1|_{\gamma=1} = 3 - \ln 2 > 0$, i.e., w is increasing in γ . Furthermore, we can formulate the second-order derivative of w with respect to γ as

$$\frac{\partial^2 w}{\partial \gamma^2} = \frac{\sqrt{m}}{(\gamma(\gamma + 2))^{\frac{5}{2}}} \left(-(\gamma + 1)^3 + \frac{1}{\gamma + 1} + 3 \ln 2(\gamma + 1) \left(\log_2(\gamma + 1) - \frac{D}{m} \right) \right). \quad (37)$$

To investigate the sign of $\frac{\partial^2 w}{\partial \gamma^2}$, we define the function

$$\Delta_2(\gamma) = -(\gamma + 1)^3 + \frac{1}{\gamma + 1} + 3 \ln 2(\gamma + 1) \log_2(\gamma + 1). \quad (38)$$

The corresponding first-order derivative of $\Delta_2(\gamma)$ is given by

$$\begin{aligned} \frac{\partial \Delta_2(\gamma)}{\partial \gamma} &= -3(\gamma + 1)^2 - \frac{1}{(\gamma + 1)^2} + 3 + 3 \ln(\gamma + 1) \leq -3(\gamma + 1)^2 - \frac{1}{(\gamma + 1)^2} + 3 + 3\gamma \\ &= -3(\gamma + 1)\gamma - \frac{1}{(\gamma + 1)^2} \leq 0. \end{aligned} \quad (39)$$

Therefore, we can obtain that $\Delta_2(\gamma)$ is decreasing in $\gamma \geq 1$ and $\Delta_2(\gamma) \leq \Delta_2(1) = 6 \ln 2 + 0.5 - 8 < 0$, $\forall \gamma \geq 1$. As a result, we have

$$\frac{\partial^2 w}{\partial \gamma^2} = \frac{\sqrt{m}}{(\gamma(\gamma + 2))^{\frac{5}{2}}} \left(\Delta_2(\gamma) - 3 \ln 2(\gamma + 1) \frac{D}{m} \right) \leq 0, \quad (40)$$

so that the term w is also concave in SNR γ .

So far, we have proved that both diagonal elements of the Hessian matrix \mathbf{H} defined in (33) are non-positive. To prove the joint concavity of w in m and γ , the final step is to guarantee a non-negative determinant for matrix \mathbf{H} . We first derive the expression for the remaining elements in the matrix \mathbf{H} , i.e.,

$$\frac{\partial^2 w}{\partial m \partial \gamma} = \frac{\partial^2 w}{\partial \gamma \partial m} = \frac{m^{-\frac{1}{2}} V^{-\frac{1}{2}} \ln 2}{2(\gamma + 1)} \left(-\frac{\mathcal{C}(\gamma) + r}{\gamma^2 + 2\gamma} + \frac{1}{\ln 2} \right). \quad (41)$$

Then, we formulate the determinant of \mathbf{H} , i.e.,

$$\det(\mathbf{H}) = \frac{\partial^2 w}{\partial m^2} \frac{\partial^2 w}{\partial \gamma^2} - \left(\frac{\partial^2 w}{\partial m \partial \gamma} \right)^2, \quad (42)$$

$$\det(\mathbf{H}) = \frac{m^{-1} \ln 2}{(\gamma^2 + 2\gamma)} \left(\underbrace{\frac{\mathcal{C}(\gamma)}{(\gamma^2 + 2\gamma) \ln 2} - \frac{3\mathcal{C}(\gamma)^2}{4(\gamma^2 + 2\gamma)} + \frac{\mathcal{C}(\gamma)}{4 \ln 2} - \frac{1}{4(\ln 2)^2} - \frac{3\mathcal{C}(\gamma)^2}{5(\gamma^2 + 2\gamma)^2}}_{\Delta_3} \right. \\ \left. + \underbrace{\frac{3r}{4 \ln 2} - \frac{3r\mathcal{C}(\gamma)}{2(\gamma^2 + 2\gamma)} - \frac{2r\mathcal{C}(\gamma)}{(\gamma^2 + 2\gamma)^2}}_{\Delta_4} \right. \\ \left. + \underbrace{\frac{2r}{(\gamma^2 + 2\gamma) \ln 2} + \frac{9r^2}{4(\gamma^2 + 2\gamma)} + \frac{2r^2}{(\gamma^2 + 2\gamma)^2} - \frac{2\mathcal{C}(\gamma)^2}{5(\gamma^2 + 2\gamma)^2}}_{\Delta_5} \right). \quad (43)$$

which can be expressed in more detail as in (43). More specifically, we have defined three terms in (43) as Δ_3 , Δ_4 and Δ_5 , respectively. Clearly, we have $\det(\mathbf{H})$ non-negative if we prove that all the three terms, i.e., Δ_3 , Δ_4 and Δ_5 , are non-negative. In the following, we will successively investigate the signs of these three terms.

Note that the term $\Delta_3 = \Delta_3(\gamma)$ is a pure function of SNR γ , while $\mathcal{C} = \log_2(1 + \gamma)$. In other words, there are no additional variables in the function $\Delta_3(\gamma)$, which motivates us to numerically determine the sign of function $\Delta_3(\gamma)$ when $\gamma \geq 1$. By studying $\frac{\partial \Delta_3}{\partial \gamma}$, we can obtain that within the region of $\gamma \in [1, \infty)$, the function $\Delta_3(\gamma)$ is monotonic. Besides, we also have $\Delta_3(1) \approx 0.0046 > 0$ and $\lim_{\gamma \rightarrow \infty} \Delta_3(\gamma) = +\infty$, which indicates that $\Delta_3(\gamma) \geq 0, \forall \gamma \geq 1$.

As for the term Δ_4 , we can show that

$$\Delta_4 = \frac{3r}{4 \ln 2} - \frac{3r\mathcal{C}(\gamma)}{2(\gamma^2 + 2\gamma)} - \frac{2r\mathcal{C}(\gamma)}{(\gamma^2 + 2\gamma)^2} = \frac{r}{\ln 2} \left(\frac{3}{4} - \frac{3 \ln(\gamma + 1)}{2(\gamma^2 + 2\gamma)} - \frac{2 \ln(\gamma + 1)}{(\gamma^2 + 2\gamma)^2} \right) \\ \stackrel{\gamma \geq 1}{\geq} \frac{r}{\ln 2} \left(\frac{3}{4} - \frac{3 \ln 2}{6} - \frac{2 \ln 2}{9} \right) \geq 0. \quad (44)$$

The above inequalities hold due to the fact that both functions $\frac{3 \ln(\gamma+1)}{2(\gamma^2+2\gamma)}$ and $\frac{2 \ln(\gamma+1)}{(\gamma^2+2\gamma)^2}$ are monotonically decreasing with respect to $\gamma \geq 1$.

Finally, for Δ_5 , we have

$$\Delta_5 > 0 \\ \Leftrightarrow r \geq \frac{2}{\ln 2(9(\gamma + 1)^2 - 1)} \left(-2\gamma^2 - 4\gamma + \sqrt{4(\gamma^2 + 2\gamma)^2 + \frac{2}{5}(9(\gamma + 1)^2 - 1) \ln^2(\gamma + 1)} \right) \\ \triangleq \Delta_6(\gamma). \quad (45)$$

Note that although the above condition seems complicated, we can still investigate the function $\Delta_6(\gamma)$ for an insight on the condition. Since $\Delta_6(\gamma)$ is a pure function of γ , we can also perform a numerical evaluation. Via letting $\frac{\partial \Delta_6}{\partial \gamma} = 0$, we can obtain the unique root $\gamma_2^* \approx 1.2408$ within the regime of $\gamma \geq 1$. And accordingly, we have that $\Delta_6(\gamma)$ is non-decreasing when $\gamma \in [\gamma_2^*, +\infty)$, while it holds $\Delta_6(\gamma) \leq \Delta_6(\gamma_2^*) \approx 0.0448$. In other words, a minimum coding rate constraint of $r \geq 0.0448$ [bits/blocklength], will be sufficient for this condition, which is also true in most practical scenarios. As a result, we have that under the condition (45), the joint concavity of w with respect to m and γ holds. Namely, in the considered high-reliability scenario, the error probability ε is jointly convex in blocklength m and SNR γ under the condition (45).

In addition, since the condition (45) lacks an intuitive physical meaning, we further derive a simple, but tight bound for the joint convexity. By comparing all three positive terms in Δ_5 , we can observe the following:

- When $r \leq \frac{8}{9 \ln 2}$, $\frac{2r}{(\gamma^2+2\gamma) \ln 2}$ is larger than $\frac{9r^2}{4(\gamma^2+2\gamma)}$. If it holds that $\frac{2r}{(\gamma^2+2\gamma) \ln 2} - \frac{2\mathcal{C}(\gamma)^2}{5(\gamma^2+2\gamma)^2} \geq 0$, then we will have $\Delta_5 \geq 0$, i.e., the joint convexity of ε in m and γ holds. More specifically, given $r \leq \frac{8}{9 \ln 2}$, we have the constraint for γ guaranteeing the convexity as

$$\begin{aligned} \frac{2r}{(\gamma^2+2\gamma) \ln 2} - \frac{2\mathcal{C}(\gamma)^2}{5(\gamma^2+2\gamma)^2} &= \frac{1}{(\gamma^2+2\gamma) \ln 2} \left(2r - \frac{2 \ln^2(\gamma+1)}{5(\gamma^2+2\gamma) \ln 2} \right) \geq 0 \\ \Leftrightarrow 2r &\geq \frac{2(\gamma+1)}{5(\gamma^2+2\gamma) \ln 2} \Leftrightarrow \gamma \geq \frac{1}{5r \ln 2}. \end{aligned} \quad (46)$$

- When $r > \frac{8}{9 \ln 2}$, we have $\frac{2r}{(\gamma^2+2\gamma) \ln 2} < \frac{9r^2}{4(\gamma^2+2\gamma)}$. Therefore, $\Delta_5 \geq 0$ holds when we have $\frac{9r^2}{4(\gamma^2+2\gamma)} - \frac{2\mathcal{C}(\gamma)^2}{5(\gamma^2+2\gamma)^2} \geq 0$, which results in the following constraint on γ :

$$\begin{aligned} \frac{9r^2}{4(\gamma^2+2\gamma)} - \frac{2\mathcal{C}(\gamma)^2}{5(\gamma^2+2\gamma)^2} &= \frac{1}{\gamma^2+2\gamma} \left(\frac{9}{4}r^2 - \frac{2 \ln^2(\gamma+1)}{5(\gamma^2+2\gamma)(\ln 2)^2} \right) \geq 0 \\ \Leftrightarrow \frac{9}{4}r^2 &\geq \frac{2(\gamma+1)}{5(\gamma^2+2\gamma) \ln^2 2} \Leftrightarrow \gamma \geq \frac{8}{45r^2 \ln^2 2}. \end{aligned} \quad (47)$$

Combining both cases together, we have that $\Delta_5 \geq 0$, when

$$\gamma \geq \max \left\{ \frac{1}{5r \ln 2}, \frac{8}{45r^2 \ln^2 2} \right\}. \quad (48)$$

Namely, compared to (45), the above condition for γ is tighter but more intuitive for the joint convexity of error probability ε with respect to m and γ .

APPENDIX B
PROOF OF LEMMA 2

The Hessian matrix of ε_i with respect to \mathbf{a} and \mathbf{b} can be written as

$$\tilde{\mathbf{H}} = \begin{pmatrix} \frac{\partial \varepsilon_i}{\partial m_i} \frac{\partial^2 m_i}{\partial a_i^2} + \frac{\partial^2 \varepsilon_i}{\partial m_i^2} \left(\frac{\partial m_i}{\partial a_i} \right)^2 & \frac{\partial \varepsilon_i}{\partial m_i \partial p_i} \frac{\partial m_i}{\partial a_i} \frac{\partial p_i}{\partial b_i} \\ \frac{\partial \varepsilon_i}{\partial m_i \partial p_i} \frac{\partial m_i}{\partial a_i} \frac{\partial p_i}{\partial b_i} & \frac{\partial \varepsilon_i}{\partial p_i} \frac{\partial^2 p_i}{\partial b_i^2} + \frac{\partial^2 \varepsilon_i}{\partial p_i^2} \left(\frac{\partial p_i}{\partial b_i} \right)^2 \end{pmatrix}.$$

To show the convexity of ε_i , we first investigate the sign of upper-left element of $\tilde{\mathbf{H}}$:

$$\begin{aligned} \frac{\partial^2 \varepsilon_i}{\partial \mathbf{a}^2} &= \frac{\partial \varepsilon_i}{\partial m_i} \frac{\partial^2 m_i}{\partial a_i^2} + \frac{\partial^2 \varepsilon_i}{\partial m_i^2} \left(\frac{\partial m_i}{\partial a_i} \right)^2 = \frac{1}{a_i^4} \frac{\partial \varepsilon_i^2}{\partial m_i^2} + \frac{2}{a_i^3} \frac{\partial \varepsilon_i}{\partial m_i} \\ &= A \left(\frac{1}{a_i} w_i \left(\frac{\partial w_i}{\partial m_i} \right)^2 - \frac{1}{a_i} \frac{\partial^2 w_i}{\partial m_i^2} - 2 \frac{\partial w_i}{\partial m_i} \right) = A \left(\underbrace{\frac{\partial w_i}{\partial m_i} \left(\frac{w_i}{a_i} \frac{\partial w_i}{\partial m_i} - 2 \right)}_{\geq 0} - \underbrace{\frac{\partial^2 w_i}{\partial m_i^2}}_{\leq 0} \right), \end{aligned} \quad (49)$$

where $A = \frac{1}{a_i^3 \sqrt{2\pi}} e^{-\frac{w_i^2}{2}}$. Therefore, the derivate is non-negative if $\frac{w_i}{a_i} \frac{\partial w_i}{\partial m_i} - 2$ is non-negative. Note that for reliable transmission, $\varepsilon_i \ll 1$, i.e., $w_i \geq Q^{-1}(0.1) \geq 1.25$. Then, we have

$$\begin{aligned} \frac{w_i}{a_i} \frac{\partial w_i}{\partial m_i} - 2 &= w_i m_i (p_i + 1) \sqrt{\frac{m_i}{p_i(p_i + 2)}} \log(p_i + 1) - 2 + w_i (p_i + 1) \sqrt{\frac{m_i}{p_i(p_i + 2)}} \frac{D_i}{m_i} \\ &\stackrel{p_i \geq 1}{\geq} 1.25(1 + 1) \sqrt{1/3} \log(2) - 2 \geq 0. \end{aligned} \quad (50)$$

Hence, the upper-left element of $\tilde{\mathbf{H}}$, i.e., the second-order derivative of ε_i with respect to \mathbf{a} is non-negative.

Next, we more specifically investigate the determinant of $\tilde{\mathbf{H}}$ in (51), in which three terms x_1 , x_2 and x_3 are defined to facilitate further analysis. According to Lemma 1, the error probability ε_i is jointly convex in m_i and $\gamma_i = p_i$. Based on the above convexity, respectively for each x_j , $j \in \{1, 2, 3\}$, we have

$$x_1 \geq 2 \left(\frac{\partial^2 \varepsilon_i}{\partial m_i^2} \frac{\partial^2 \varepsilon_i}{\partial p_i^2} - \left(\frac{\partial^2 \varepsilon_i}{\partial m_i \partial p_i} \right)^2 \right) \stackrel{\text{Lemma 1}}{\geq} 0, \quad (52)$$

$$x_2 \geq w_i \sqrt{\frac{m_i}{1 - \frac{1}{(1+p_i)^2}}} \left(\frac{1}{p_i + 1} - \frac{\log(p_i + 1)}{(p_i^2 + 2p_i)(p_i + 1)} \right) - 1 \geq 1.25 \frac{\sqrt{6}}{2} \left(\frac{1}{2} - \frac{\log 2}{6} \right) - 1 \geq 0, \quad (53)$$

and

$$x_3 \geq \frac{w_i}{a_i} \frac{\partial w_i}{\partial m_i} - 2 \geq 0. \quad (54)$$

Therefore, we have $x_j \geq 0, \forall j = 1, 2, 3$ and all other components in (51) are non-negative, i.e.,

$$\begin{aligned}
\det(\tilde{\mathbf{H}}) &= \frac{4b_i^2}{a_i^4} \frac{\partial^2 \varepsilon_i}{\partial m_i^2} \frac{\partial^2 \varepsilon_i}{\partial p_i^2} - \frac{2b_i}{a_i^2} \left(\frac{\partial^2 \varepsilon_i}{\partial m_i \partial p_i} \right)^2 + \frac{2}{a^4} \frac{\partial^2 \varepsilon_i}{\partial m_i^2} \frac{\partial \varepsilon_i}{\partial p_i} + \frac{8b_i^2}{a_i^3} \frac{\partial^2 \varepsilon_i}{\partial p_i^2} \frac{\partial \varepsilon_i}{\partial m_i} + \frac{4}{a_i^3} \frac{\partial \varepsilon_i}{\partial m_i} \frac{\partial \varepsilon_i}{\partial p_i} \\
&= \frac{b_i}{a_i^2} \left(\underbrace{2 \frac{b_i}{a_i^2} \frac{\partial^2 \varepsilon_i}{\partial m_i^2} \frac{\partial^2 \varepsilon_i}{\partial p_i^2} - 2 \left(\frac{\partial \varepsilon_i}{\partial m_i \partial p_i} \right)^2}_{x_1} \right) + \frac{4}{a_i^3} \underbrace{\frac{\partial \varepsilon_i}{\partial m_i} \frac{\partial \varepsilon_i}{\partial p_i}}_{\geq 0} \\
&\quad + \frac{A^2}{a_i^3} \left(4b_i^2 w_i \underbrace{\left(\frac{\partial w_i}{\partial m_i} \right)^2 \frac{\partial w_i}{\partial p_i}}_{\geq 0} \underbrace{\left(\frac{2w_i}{a_i} \frac{\partial w_i}{\partial p_i} - 2 \right)}_{x_2} \right) + 8b_i^2 \underbrace{\left(-\frac{\partial^2 w_i}{\partial m_i^2} \right) \frac{\partial w_i}{\partial p_i}}_{\geq 0} \underbrace{\left(\frac{2w_i}{a_i} \frac{\partial w_i}{\partial p_i} - 1 \right)}_{\geq x_2} \\
&\quad + \frac{w_i}{a_i} \underbrace{\left(\frac{\partial w_i}{\partial p_i} \right)^2 \frac{\partial w_i}{\partial m_i}}_{\geq 0} \underbrace{\left(\frac{2b_i^2 w_i}{a_i} \frac{\partial w_i}{\partial m_i} - 1 \right)}_{x_3} \\
&\quad + \frac{2}{a_i} \underbrace{\left(-\frac{\partial^2 w_i}{\partial p_i^2} \right) \frac{\partial w_i}{\partial m_i}}_{\geq 0} \underbrace{\left(\frac{3b_i^2 w_i}{a_i} \frac{\partial w_i}{\partial m_i} - 1 \right)}_{\geq x_3} + \frac{12b_i^2}{a_i} \underbrace{\frac{\partial^2 w_i}{\partial p_i^2} \frac{\partial^2 w_i}{\partial m_i^2}}_{\geq 0} \\
&\geq \frac{b_i}{a_i^2} x_1 + \frac{A^2}{a_i^3} \left(\left(\left(\frac{\partial w_i}{\partial m_i} \right)^2 \frac{\partial w_i}{\partial p_i} - \frac{\partial^2 w_i}{\partial m_i^2} \frac{\partial w_i}{\partial p_i} \right) x_2 + \left(\left(\frac{\partial w_i}{\partial p_i} \right)^2 \frac{\partial w_i}{\partial m_i} - \frac{\partial^2 w_i}{\partial p_i^2} \frac{\partial w_i}{\partial m_i} \right) x_3 \right)
\end{aligned} \tag{51}$$

it holds that $\det \tilde{\mathbf{H}} \geq 0$.

As a result, ε_i is jointly convex in \mathbf{b} and \mathbf{a} .

REFERENCES

- [1] M. Bennis, M. Debbah, and H. V. Poor, "Ultra-reliable and Low-Latency Wireless Communication: Tail, Risk, and Scale," *Proceedings of the IEEE*, vol. 106, no. 10, pp. 1834–1853, 2018.
- [2] Z. Meng, C. She, G. Zhao, and D. De Martini, "Sampling, Communication, and Prediction Co-Design for Synchronizing the Real-World Device and Digital Model in Metaverse," 2022. [Online]. Available: <https://arxiv.org/abs/2208.04233>
- [3] C. She, C. Yang, and T. Q. S. Quek, "Radio Resource Management for Ultra-Reliable and Low-Latency Communications," *IEEE Communications Magazine*, vol. 55, no. 6, pp. 72–78, 2017.
- [4] X. Chen, D. W. K. Ng, W. Yu, E. G. Larsson, N. Al-Dhahir, and R. Schober, "Massive Access for 5G and Beyond," *IEEE Journal on Selected Areas in Communications*, vol. 39, no. 3, pp. 615–637, 2021.
- [5] Y. Polyanskiy, H. V. Poor, and S. Verdú, "Channel Coding Rate in the Finite Blocklength Regime," *IEEE Transactions on Information Theory*, vol. 56, no. 5, pp. 2307–2359, 2010.
- [6] Y. Polyanskiy, H. V. Poor, and S. Verdú, "Dispersion of the Gilbert-Elliott channel," in *2009 IEEE International Symposium on Information Theory*, 2009, pp. 2209–2213.

- [7] W. Yang, G. Durisi, T. Koch, and Y. Polyanskiy, "Quasi-Static Multiple-Antenna Fading Channels at Finite Blocklength," *IEEE Transactions on Information Theory*, vol. 60, no. 7, pp. 4232–4265, 2014.
- [8] W. Yang, G. Caire, G. Durisi, and Y. Polyanskiy, "Finite-blocklength channel coding rate under a long-term power constraint," in *2014 IEEE International Symposium on Information Theory*, 2014, pp. 2067–2071.
- [9] Y. Hu, J. Gross, and A. Schmeink, "On the Capacity of Relaying With Finite Blocklength," *IEEE Transactions on Vehicular Technology*, vol. 65, no. 3, pp. 1790–1794, 2016.
- [10] —, "On the Performance Advantage of Relaying Under the Finite Blocklength Regime," *IEEE Communications Letters*, vol. 19, no. 5, pp. 779–782, 2015.
- [11] Y. Hu, A. Schmeink, and J. Gross, "Blocklength-Limited Performance of Relaying Under Quasi-Static Rayleigh Channels," *IEEE Transactions on Wireless Communications*, vol. 15, no. 7, pp. 4548–4558, 2016.
- [12] —, "Optimal Scheduling of Reliability-Constrained Relaying System Under Outdated CSI in the Finite Blocklength Regime," *IEEE Transactions on Vehicular Technology*, vol. 67, no. 7, pp. 6146–6155, 2018.
- [13] Z. Xiang, W. Yang, Y. Cai, Z. Ding, Y. Song, and Y. Zou, "NOMA-Assisted Secure Short-Packet Communications in IoT," *IEEE Wireless Communications*, vol. 27, no. 4, pp. 8–15, 2020.
- [14] X. Lai, T. Wu, Q. Zhang, and J. Qin, "Average Secure BLER Analysis of NOMA Downlink Short-Packet Communication Systems in Flat Rayleigh Fading Channels," *IEEE Transactions on Wireless Communications*, pp. 1–1, 2020.
- [15] F. Ghanami, G. A. Hodtani, B. Vucetic, and M. Shirvanimoghaddam, "Performance Analysis and Optimization of NOMA With HARQ for Short Packet Communications in Massive IoT," *IEEE Internet of Things Journal*, vol. 8, no. 6, pp. 4736–4748, 2021.
- [16] O. L. Alcaraz Lopez, E. M. G. Fernandez, R. D. Souza, and H. Alves, "Wireless Powered Communications With Finite Battery and Finite Blocklength," *IEEE Transactions on Communications*, vol. 66, no. 4, pp. 1803–1816, 2018.
- [17] B. Makki, T. Svensson, and M. Zorzi, "Wireless Energy and Information Transmission Using Feedback: Infinite and Finite Block-Length Analysis," *IEEE Transactions on Communications*, vol. 64, no. 12, pp. 5304–5318, 2016.
- [18] C. Wang, Z. Li, H. Zhang, D. W. K. Ng, and N. Al-Dhahir, "Achieving Covertness and Security in Broadcast Channels with Finite Blocklength," *IEEE Transactions on Wireless Communications*, pp. 1–1, 2022.
- [19] K. Singh, M.-L. Ku, and M. F. Flanagan, "Energy-Efficient Precoder Design for Downlink Multi-User MISO Networks With Finite Blocklength Codes," *IEEE Transactions on Green Communications and Networking*, vol. 5, no. 1, pp. 160–173, 2021.
- [20] Y. Zhu, Y. Hu, A. Schmeink, and J. Gross, "Energy Minimization of Mobile Edge Computing Networks with HARQ in the Finite Blocklength Regime," *IEEE Transactions on Wireless Communications*, pp. 1–1, 2022.
- [21] M. Y. Abdelsadek, Y. Gadallah, and M. H. Ahmed, "A Critical MTC Resource Allocation Approach for LTE Networks With Finite Blocklength Codes," *IEEE Transactions on Vehicular Technology*, vol. 69, no. 5, pp. 5598–5609, 2020.
- [22] X. Sun, S. Yan, N. Yang, Z. Ding, C. Shen, and Z. Zhong, "Short-Packet Downlink Transmission With Non-Orthogonal Multiple Access," *IEEE Transactions on Wireless Communications*, vol. 17, no. 7, pp. 4550–4564, 2018.
- [23] Y. Hu, M. Ozmen, M. C. Gursoy, and A. Schmeink, "Optimal Power Allocation for QoS-Constrained Downlink Multi-User Networks in the Finite Blocklength Regime," *IEEE Transactions on Wireless Communications*, vol. 17, no. 9, pp. 5827–5840, 2018.
- [24] S. He, Z. An, J. Zhu, J. Zhang, Y. Huang, and Y. Zhang, "Beamforming Design for Multiuser uRLLC With Finite Blocklength Transmission," *IEEE Transactions on Wireless Communications*, vol. 20, no. 12, pp. 8096–8109, 2021.
- [25] L. Yuan, N. Yang, F. Fang, Q. Du, and Z. Zheng, "Optimal Power Allocation for Finite Blocklength Cooperative NOMA With Coordinated Direct and Relay Transmission," *IEEE Wireless Communications Letters*, vol. 11, no. 3, pp. 523–527, 2022.

- [26] T.-X. Zheng, H.-M. Wang, D. W. K. Ng, and J. Yuan, "Physical-Layer Security in the Finite Blocklength Regime Over Fading Channels," *IEEE Transactions on Wireless Communications*, vol. 19, no. 5, pp. 3405–3420, 2020.
- [27] B. Makki, T. Svensson, and M. Zorzi, "Finite Block-Length Analysis of Spectrum Sharing Networks Using Rate Adaptation," *IEEE Transactions on Communications*, vol. 63, no. 8, pp. 2823–2835, 2015.
- [28] —, "Finite Block-Length Analysis of the Incremental Redundancy HARQ," *IEEE Wireless Communications Letters*, vol. 3, no. 5, pp. 529–532, 2014.
- [29] X. Lai, Q. Zhang, and J. Qin, "Cooperative NOMA Short-Packet Communications in Flat Rayleigh Fading Channels," *IEEE Transactions on Vehicular Technology*, vol. 68, no. 6, pp. 6182–6186, 2019.
- [30] B. Yu, Y. Cai, D. Wu, and Z. Xiang, "Average Age of Information in Short Packet Based Machine Type Communication," *IEEE Transactions on Vehicular Technology*, vol. 69, no. 9, pp. 10 306–10 319, 2020.
- [31] H. Ren, C. Pan, Y. Deng, M. ElKashlan, and A. Nallanathan, "Joint Power and Blocklength Optimization for URLLC in a Factory Automation Scenario," *IEEE Transactions on Wireless Communications*, vol. 19, no. 3, pp. 1786–1801, 2020.
- [32] C. She, C. Yang, and T. Q. S. Quek, "Joint Uplink and Downlink Resource Configuration for Ultra-Reliable and Low-Latency Communications," *IEEE Transactions on Communications*, vol. 66, no. 5, pp. 2266–2280, 2018.
- [33] C. Sun, C. She, C. Yang, T. Q. S. Quek, Y. Li, and B. Vucetic, "Optimizing Resource Allocation in the Short Blocklength Regime for Ultra-Reliable and Low-Latency Communications," *IEEE Transactions on Wireless Communications*, vol. 18, no. 1, pp. 402–415, 2019.
- [34] M. Haghifam, M. Robat Mili, B. Makki, M. Nasiri-Kenari, and T. Svensson, "Joint Sum Rate and Error Probability Optimization: Finite Blocklength Analysis," *IEEE Wireless Communications Letters*, vol. 6, no. 6, pp. 726–729, 2017.
- [35] S. Han, X. Xu, Z. Liu, P. Xiao, K. Moessner, X. Tao, and P. Zhang, "Energy-Efficient Short Packet Communications for Uplink NOMA-Based Massive MTC Networks," *IEEE Transactions on Vehicular Technology*, vol. 68, no. 12, pp. 12 066–12 078, 2019.
- [36] A. Lancho, J. Ostman, G. Durisi, T. Koch, and G. Vazquez-Vilar, "Saddlepoint Approximations for Short-Packet Wireless Communications," *IEEE Transactions on Wireless Communications*, vol. 19, no. 7, pp. 4831–4846, 2020.
- [37] Y. Hu, Y. Zhu, M. C. Gursoy, and A. Schmeink, "SWIPT-Enabled Relaying in IoT Networks Operating With Finite Blocklength Codes," *IEEE Journal on Selected Areas in Communications*, vol. 37, no. 1, pp. 74–88, 2019.
- [38] Y. Hu, M. C. Gursoy, and A. Schmeink, "Efficient transmission schemes for low-latency networks: Noma vs. relaying," in *Proceedings of the 2017 IEEE 28th Annual International Symposium on Personal, Indoor, and Mobile Radio Communications (PIMRC)*, 2017, pp. 1–6.
- [39] A. Avranas, M. Kountouris, and P. Ciblat, "Energy-Latency Tradeoff in Ultra-Reliable Low-Latency Communication With Retransmissions," *IEEE Journal on Selected Areas in Communications*, vol. 36, no. 11, pp. 2475–2485, 2018.
- [40] Y. Polyanskiy, H. V. Poor, and S. Verdú, "Dispersion of gaussian channels," in *Proceedings of the 2009 IEEE International Symposium on Information Theory*, 2009, pp. 2204–2208.
- [41] B. Han, Y. Zhu, Z. Jiang, M. Sun, and H. D. Schotten, "Fairness for Freshness: Optimal Age of Information Based OFDMA Scheduling With Minimal Knowledge," *IEEE Transactions on Wireless Communications*, vol. 20, no. 12, pp. 7903–7919, 2021.
- [42] P. Tseng, "Convergence of a Block Coordinate Descent Method for Nondifferentiable Minimization," *Journal of Optimization Theory and Applications*, vol. 109, no. 3, pp. 475–494, 2001.
- [43] Y. Hu, A. Schmeink, and J. Gross, "Blocklength-Limited Performance of Relaying Under Quasi-Static Rayleigh Channels," *IEEE Transactions on Wireless Communications*, vol. 15, no. 7, pp. 4548–4558, 2016.
- [44] C. Pan, H. Ren, Y. Deng, M. ElKashlan, and A. Nallanathan, "Joint Blocklength and Location Optimization for URLLC-Enabled UAV Relay Systems," *IEEE Communications Letters*, vol. 23, no. 3, pp. 498–501, 2019.

- [45] A. Agarwal, A. K. Jagannatham, and L. Hanzo, "Finite Blocklength Non-Orthogonal Cooperative Communication Relying on SWIPT-Enabled Energy Harvesting Relays," *IEEE Transactions on Communications*, vol. 68, no. 6, pp. 3326–3341, 2020.